THE JOURNAL OF PHYSICAL CHEMISTRY C

Article

Multiwall Carbon Nanotubes Decorated with Copper Nanoparticles: Effect on the Photocurrent Response

M. Scarselli, C. Scilletta, F. Tombolini, P. Castrucci, M. Diociaiuti, S. Casciardi, E. Gatto, M. Venanzi, and M. De Crescenzi

J. Phys. Chem. C, **2009**, 113 (14), 5860-5864• DOI: 10.1021/jp809944d • Publication Date (Web): 18 March 2009

Multiwall Carbon Nanotubes Decorated with Copper Nanoparticles: Effect on the Photocurrent Response

M. Scarselli,*,† C. Scilletta,†,⊥ F. Tombolini,† P. Castrucci,† M. Diociaiuti,‡ S. Casciardi,§ E. Gatto,|| M. Venanzi,|| and M. De Crescenzi†

Physics Department, CNISM Unit, University of Rome Tor Vergata, 00133 Rome, Italy, Technology and Health Department, Istituto Superiore di Sanità, 00161 Rome, Italy, Department of Occupational Hygiene, National Institute of Prevention and Safety at Workplace (ISPESL), 00040 Monte Porzio Catone, Italy, Science and Chemical Technologies Department, University of Rome Tor Vergata, 00133 Rome, Italy, and Istituto dei Sistemi Complessi, CNR, 00016 Monterotondo Scalo, Italy

Received: July 3, 2008; Revised Manuscript Received: February 11, 2009

Photocurrent generation measured with an electrochemical cell on carbon nanotubes has been obtained mainly from single-walled nanostructures. In fact, multiwall carbon nanotubes (MWCNTs) were not expected to show analogous low-dimensional effects, due to their close similarity to metallic graphite. Recently we reported on the ability of MWCNTs to generate photocurrent in the visible and ultraviolet spectral range. In this paper we show a significant enhancement in the photocurrent generation when the walls of the MWCNTs were decorated with dispersed Cu nanoparticles. This result is of particular relevance for photovoltaic nanodevices and solar energy conversion applications.

Introduction

Photovoltaics has usually relied on semiconductor p−n junctions mainly derived from silicon and III−V semiconductors.[1] The foremost limiting factor in the photoconversion efficiency is the loss of the excess energy that the electrons receive when excited above the conduction band minimum in thermal lattice vibrations. Recent studies have envisaged the possibility of achieving high conversion efficiencies by using new three-dimensional confined material systems such as nanocrystallites or quantum dots.[2,3] In addition, one-dimensional nanostructures, such as ZnO,[4] Si nanowires,[5,6] CdSe,[7,8] and single-wall (SWCNTs)[9−14] and multiwall carbon nanotubes (MWCNTs)[15−17] proved to be attractive platforms for photovoltaic applications. Above all, the one-dimensional carbon nanotube superstructure offers the particular advantage of accessing the largest active surface for photon absorption and thus harvesting solar energy. The presence of extended, delocalized π-electron states is, indeed, very useful for charge transfer and transport.[12] It has been recently shown that the dispersion of semiconducting quantum dots[18,19] or metallic (Au) nanoparticles[20] on the CNTs sidewalls yields a significant enhancement in the photoconversion efficiency. In this regard, a great deal of research has been devoted to trying to understand the modification of the electronic properties of carbon nanotubes/metal hybrids as a function of the type, size, and shape of the dispersed metal nanoparticles.[21−24] Theoretical and experimental data obtained from metal-coated nanotubes demonstrate that metals are likely to mechanically stabilize and passivate defect sites on the CNT surface. In the case of 3d elements on SWCNTs,[22] it has been observed that the nature of the system's contact resistance can vary substantially and a sizable charge transfer from the metal to the carbon has been theoretically predicted. The charge transfer affects not only the 4s electrons but also the 3d electrons of copper.[25] Indeed, studies performed on Cu nanoparticles have demonstrated that, by reducing the size of Cu-nanoparticles, there is an important loss of metallicity followed by a localization of the electronic levels similar to that expected in a semiconducting material.[26,27] Therefore, it is possible to vary the electronic properties of the metal nanoparticles and increase the total absorption of the carbon nanotube/metal nanohybrids. In this research field, of equal interest are multiwall carbon nanotubes (MWCNTs), in which the presence of numerous concentric cylindrical walls provides additional pathways for the flow of photogenerated charge carriers. The obvious challenge is to use a MWCNTs network in a solar cell as a scaffold to anchor light-harvesting metal nanoparticles and facilitate the electron transport to the collecting electrode surface.

Recently, we showed photoelectrochemical measurements that demonstrate the ability of MWCNTs to generate photocurrent. The main result was an incident photon-to-current efficiency (IPCE)[28] of 7% at 3.54 eV[15,16] for multiwall carbon nanotubes, 30 times more intense than the efficiency measured in SWCNTs (0.2%).[14]

In this work we show that a remarkable increase in the photoelectrochemically generated current signal from the deposition of Cu nanoparticles on the sidewalls of MWCNTs can be obtained and the effect can be detected over the entire visible and near-ultraviolet energy range. In fact, the photoactive metal nanoparticles greatly enhance the intrinsic ability of MWCNTs to behave as an efficient low-dimensional media for generating e-h carriers. The reported hybrid system seems to be as promising as that obtained from functionalization with organic molecules.[29,30]

* To whom correspondence should be addressed. Phone: + 39 0672594116. Fax: +39 062023507. E-mail: manuela.scarselli@roma2.infn.it.
† Physics Department, CNISM Unit, University of Rome Tor Vergata.
⊥ Istituto dei Sistemi Complessi.
‡ Technology and Health Department, Istituto Superiore di Sanità.
§ Department of Occupational Hygiene, National Institute of Prevention and Safety at Workplace (ISPESL).
|| Science and Chemical Technologies Department, University of Rome Tor Vergata.

10.1021/jp809944d CCC: $40.75
Published on Web 03/18/2009

Experimental Methods

Nanotube Growth Process. A silicon dioxide (SiO_2) substrate (Siltronix) of 100 nm thermally grown on Si(100) was used as a starting substrate for the carbon nanotube growth.

The substrate was inserted into the growth chamber operating in ultrahigh vacuum conditions (UHV) and iron (Fe) catalyst was deposited, at room temperature, on the clean oxide substrate by thermal evaporation from a tungsten basket at a base pressure of 1×10^{-8} Torr during the deposition.

The nominal Fe thickness estimated with a quartz microbalance was about 1.00 ± 0.01 nm. Subsequently, carbon nanotubes were grown by thermal chemical vapor deposition (CVD) in acetylene (C_2H_2) atmosphere (700 Torr of pressure, for 30 min) while keeping the substrate covered by Fe nanoislands at $T =$ 800 °C during the growth.

Cu Nanoparticle Deposition. Soon after the growth of MWCNTs, we deposited Cu by thermal evaporation from a tungsten crucible in the same growth chamber at a base pressure of 1×10^{-8} Torr. The nominal Cu thickness, estimated with a quartz microbalance, was about 0.10 ± 0.01nm.

Scanning Electron Microscopy (SEM) and Transmission Electron Microscopy (TEM). SEM and TEM measurements were used to characterize the morphology, purity, and internal structure of the carbon nanotubes. SEM images were recorded with a Cambridge 360 SteroScan apparatus (10 keV) on MWCNTs and Cu-MWCNTs samples.

TEM measurements were performed in a FEI TECNAI 12 (120 keV) apparatus equipped with an energy filter (GATAN GIF model) and a Peltier cooled SSC (slow scan charged-coupled device) multiscan camera (794 IF model). A droplet of the raw synthesis product diluted in isopropyl alcohol was used to disperse the nanotubes on a gold TEM grid (mesh 1000). Most of the reaction products are thereby located next to or bridged between two gold wires.

X-ray Photoelectron Spectroscopy. X-ray photoelectron spectra were collected from both MWCNTs and Cu-MWCNTs samples. The data were measured with a semi-imaging analyzer MAC 2 (Riber Instruments) operating in the constant pass energy mode (with a total energy resolution of 1.0 eV), using non-monochromatized Mg Kα (1253.6 eV) radiation source (9 kV, 700 W). The distance between the sample and the anode was about 40 mm, the illumination area was about 5×5 mm^2 and the takeoff angle between the sample surface and the photoelectron energy analyzer was kept fixed at 45°. The energy scale with reference to the binding energy of the C1s was calibrated at 284.7 eV with respect to the Fermi level.[31] Extended energy distribution spectra were first recorded, followed by high-resolution scans over the Cu2p photoelectron binding energy region. XPS spectra were analyzed by using a standard Gaussian curve fit routine with a Shirley background subtraction;[32] the quality of the fit was evaluated by using the χ^2 minimization test.

Photoelectrochemical Measurements. Photoelectrochemical measurements on MWCNTs/SiO_2 and Cu-MWCNTs/SiO_2 electrodes were carried out in a conventional three-arm electrochemical cell by using platinum (Pt) wire as a counter electrode and a standard calomel electrode (SCE) as a reference electrode. A 0.5 M NaI and 0.01 M I_2 in acetonitrile solution was used as electrolyte. A 200W Xe lamp (Osram) was employed as excitation source ($\lambda > 300$ nm). The intensity of the light near the electrode surface was estimated by azobenzene actinometry.[33] Photocurrent measurements were carried out with use of the Xe lamp equipped with a monochromator to select the incident excitation wavelength and a PG-310 (HEKA ELEKTRONIK) potentionstat to measure the generated current. The intensity of the photocurrent signal was normalized to the excited area covered by the nanotubes.

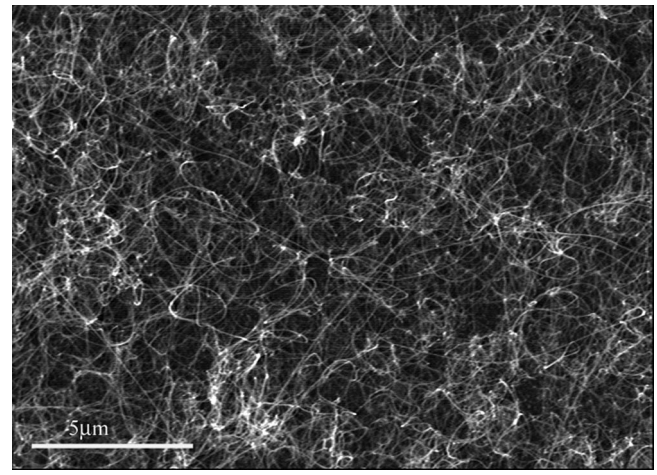

Figure 1. SEM image obtained from MWCNT after Cu deposition.

Absorption Measurements. Absorption measurements on MWCNTs/SiO_2 and Cu-MWCNTs/SiO_2 electrodes were carried out with a commercial apparatus (Perkin-Elmer, LAMBDA 15). The signal was obtained by irradiating a conventional 1 mm quartz cuvette containing the synthesis product diluted in isopropyl alcohol.

Results and Discussion

The MWCNTs were first studied with SEM and TEM. In this regard, both techniques made it possible to obtain morphological and structural information on the carbon nanotubes before and after Cu nanoparticle deposition.

SEM images obtained on both MWNTs and Cu-MWCNTs ruled out the presence of carbonaceous and/or graphitic reaction products. Nanotubes grew homogeneously on all the substrates and did not show a preferential orientation with respect to the substrate, as shown in Figure 1. The best spatial resolution was insufficient to clearly identify the presence of Cu-nanoparticles on the nanotube surface. This task was accomplished by TEM analysis, as shown in Figure 2a, which displays a TEM image obtained on a group of free-standing nanotubes after Cu deposition. Several nanoparticles formed at the CNT's outer walls could be identified as isolated or agglomerated and randomly distributed on the CNT walls. The composition of the nanoparticles was established by performing the energy loss spectroscopy (EELS) analysis close to $L_{2,3}$ ionization edges on single particles (data not shown). The obtained spectra indicated that nanoparticles were made of copper. In particular, Figure 2b, reports a high-resolution TEM image obtained on a single MWCNT decorated with the nanoparticles; their shape was mostly faceted with an average diameter of about 6.0 ± 1.0 nm.

XPS studies were performed to characterize the electronic properties of the Cu nanoparticles deposited on the nanotube walls. Figure 3, reports the line spectrum of the Cu 2p core levels. A nonlinear curve fitting of the observed intensities evidenced two main features corresponding to the Cu $2p_{3/2}$ and Cu $2p_{1/2}$ binding energies, respectively, while the energy difference between the reported energies is about 20 eV.[31] Interestingly, the Cu2p spectrum appeared as a single line with no additional shifted structures due to the presence of oxidized components.

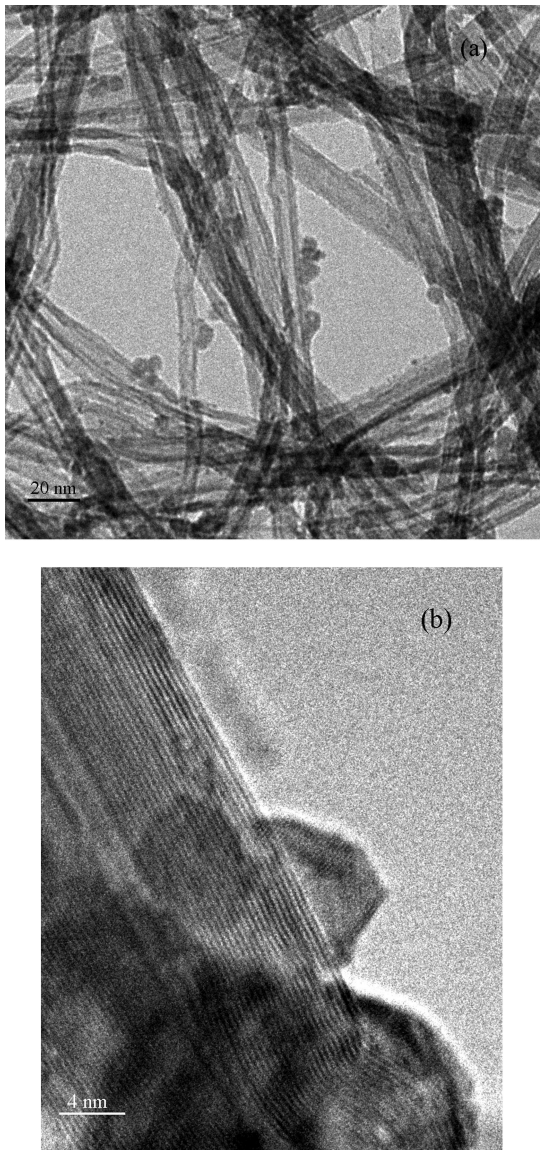

Figure 2. TEM images obtained on MWCNT after Cu deposition. (a) TEM image obtained of a group of free-standing nanotubes after Cu deposition. Several Cu nanoparticles attached to the CNT's outer walls could be identified from the image. (b) High-resolution image obtained on a single MWCNT decorated with Cu nanoparticles randomly distributed on the external walls of the nanotube.

Finally the MWCNTs electrode performance was obtained by recording the photocurrent density at different incident photon energies. A sketch of the apparatus together with an illustration of the electron transfer from the photoexcited Cu-nanoparticles and the MWCNT is reported in Scheme 1. In the proposed scheme the electron is collected at the electrode surface and the hole is scavenged by the electrolyte in solution giving rise to a net anodic current. The anodic character of the photocurrent signal evidenced by the on−off current cycle reported in Figure 4 indicates the electronic character of the charge carriers.

The IPCE[28] obtained from MWCNTs and Cu-MWCNTs at different photon excitation energy is reported in Figure 5. The signal obtained on the bare SiO_2 substrate turned out to be structureless and of negligeable intensity throughout the photon energy range investigated and was not inserted in the figure.

We observed that the IPCE, at the emission maximum located at 3.2 eV, reached 1% for bare MWCNTs while we measured a sizable increase up to 4.5% for Cu decorated multiwall CNTs. The inset of Figure 5 reports the absorption characteristics of

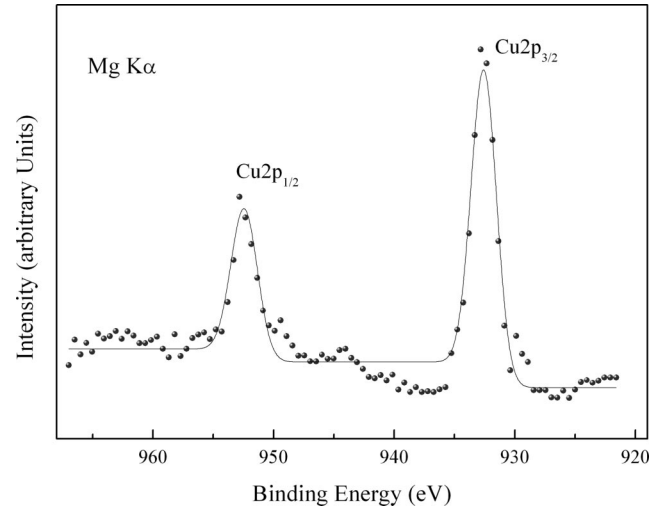

Figure 3. XPS (Mg Kα, $h\nu = 1253.6$ eV) Cu2p core level spectrum obtained on MWCNT after Cu deposition. Solid circles are experimental data (●); the solid line is the fitting curve obtained summing up the Gaussian components computed by the nonlinear curve fit procedure.

SCHEME 1: Light-Induced Charge Separation in the Photoelectrochemical Cell Based on Cu-MWCNTs[a]

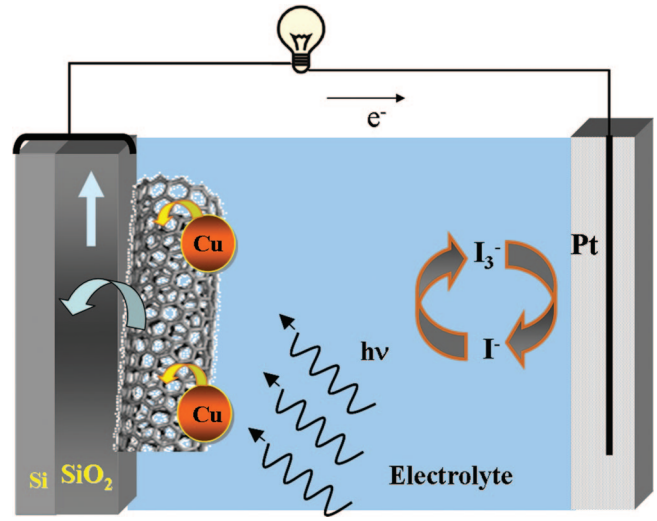

[a] In the proposed scheme the electron is collected at the electrode surface and the hole is scavenged by the electrolyte in solution giving rise to a net anodic current. The anodic character of the photocurrent signal evidenced by the on−off current cycle reported in Figure 4 indicates the electronic nature of the charge carriers. Electrolyte: NaI 0.5 M and I_2 0.01 M in acetonitrile.

both MWCNT and Cu-MWCNT obtained in solution that follow the observed photocurrent behavior.

In Figure 6 we report the current densities measured for MWCNTs and Cu-MWCNTs under dark and illumination (at a wavelength of 400 nm) as a function of the applied cell voltage. It was observed that in the presence of Cu nanoparticles there were much better photocurrent response than that with pristine MWCNTs. The maximum of the IPCE around 3.2 eV for MWCNTs confirms the result reported in earlier experiments performed on similar MWCNT samples.[16,17] In addition, we have already demonstrated that different IPCE values ranging from 1.0% to 7% (at a wavelength of 350 nm) can be obtained covering the most defective to the best MWCNTs sample.[16,17]

Accordingly, in the present work we were very careful to maintain reproducible experimental conditions during the

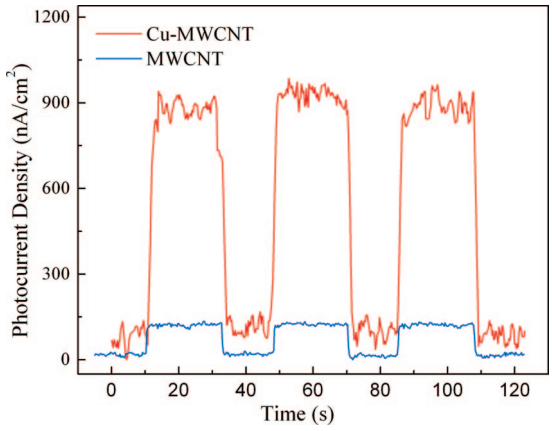

Figure 4. Typical on−off current cycle in MWCNTs (blue line) and Cu-MWCNTs (red line) obtained at $\lambda = 400$ nm incident photon wavelength.

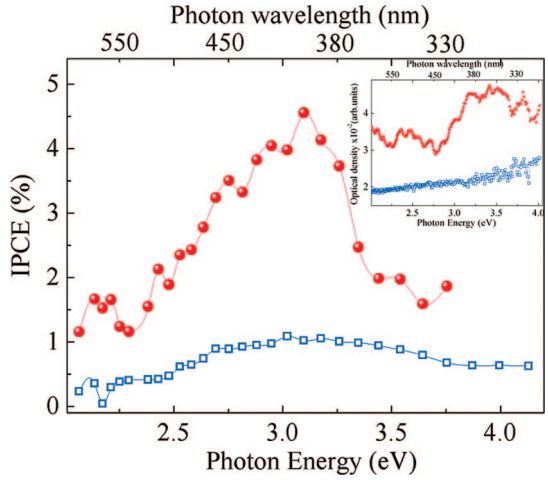

Figure 5. Photocurrent action spectra of MWCNTs (open squares, □) and CuMWCNTs (solid circles, ●), obtained as a function of incident photon energy $\lambda > 280$ nm (CE is Pt; electrolyte is NaI 0.5 M and I_2 0.01 M in acetonitrile, 12 mV applied cell voltage). IPCE is determined by using the equation of ref 28. Inset: Absorption spectra of MWCNTs and CuMWCNTs performed in solution. Note that the absorption resembles the action spectrum of the photocurrent density.

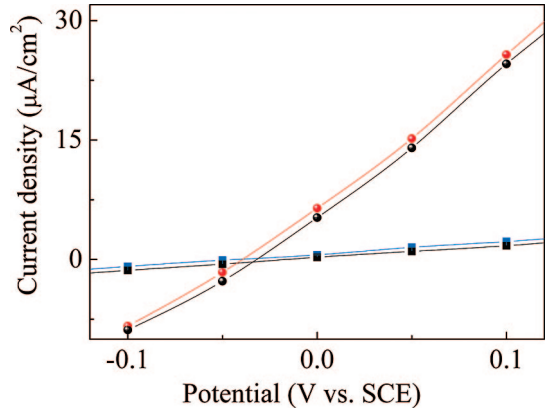

Figure 6. Photocurrent density signal obtained from incident light ($\lambda = 400$ nm) on both MWCNTs (solid squares: light, blue; and dark, black) and Cu-MWCNTs (full circles: light, red; and dark, black) as a function of the applied cell voltage.

MWCNTs and the Cu-MWCNTs synthesis. The TEM in fact showed that nanotubes have similar structural properties such as the same average number of walls and defects.

The presence of a photocurrent signal is a clear-cut indication that MWCNTs act as photoconductive material. This property is essential for the conversion of light into electricity as upon illumination a fast charge separation and a slow charge recombination is required. In charge-separated species lifetimes of the order of microseconds have been evaluated in photocurrent generation in SWCNTs.[11] Longer lifetimes are expected for MWCNTs than for SWCNTs, due to an enhanced delocalization and percolation of the electrons inside the concentric tubes which decelerate the recombination's decay dynamics.

Although MWCNTs should mimic the electronic properties of metallic graphite, the quantum confinement of the charged carriers within the nanotubes creates strongly bound excitons[16,17] which dramatically modify the electronic behavior. This finding is supported by the presence of van Hove singularities that produce highly localized states in the infrared and visible energy region as theoretically[34] predicted and evidenced by energy loss measurements.[17] Thus the broad photocurrent feature located at 3.3 eV should be ascribed to e-h excitations coming from the van Hove singularities of each concentric cylindrical wall. The presence of both semiconducting and metallic walls inside the same nanotube gives rise to localized Schottky barriers thus increasing the carriers' recombination time. In addition to this picture the whole system made up of metallic and semiconducting nanotubes[35] gives rise to the formation of localized Schottky barriers between one nanotube and another.[36] This favors the diffusion of the optically excited electrons to the electrode and the interaction of the optically excited holes with the electrolyte.

The increase in the overall photocurrent signal for Cu-MWCNTs (reported in Figure 5 as IPCE) demonstrates the ability of Cu nanoparticles to significantly modify the electronic properties of the entire hybrid system. Copper is known to be a good electron donor upon photoexcitation. Therefore, the photocurrent signal enhancement indicates that additional electrons coming from the Cu nanoparticles are efficiently transferred to the numerous concentric cylindrical walls of carbon nanotubes which offer more pathways for the flow of photogenerated charge carriers.

Conclusion

The combination of MWCNTs with electron-donor groups constituted by small metal nanoparticles is an innovative concept in the context of photovoltaic systems. MWCNTs are somewhat easier to process than SWNTs, because they are less prone to forming tight bundles. Due to the presence of numerous concentric cylindrical tubes, MWCNTs should be even more suitable for achieving charge transfer and transport than SWCNTs are. MWCNTs interact similarly to SWCNTs with light showing a peculiar photovoltaic property because they operate as unconventional "Schottky barrier diodes" in which two diode actions occur, one inside the nanotube (between the metallic and semiconducting walls) and the other between the nanotube/nanotube junctions. In addition, the ability of Cu nanodots to optically absorb both in the infrared and in the visible range makes this system more suitable for light-energy conversion applications than CNTs functionalized with organic molecules due to higher resistance to continuous optical excitation. [29,30]

Whereas other systems may have shown higher efficiency, the deposition method presented here can be used for other metallic nanoparticles and can be considered complementary to those already existing. Since the problem of solar-energy conversion is so important, we believe that the promising increment in the IPCE obtained from the Cu decorated

MWCNTs of our experiments deserves further investigation. This would include studies on more efficient methods for packing MWCNTs into thin films once each nanotube has been decorated with metallic nanoparticles.

Acknowledgment. The authors thank the Italian Foreign Affairs Ministry through 2008 Promotion and Cultural Cooperation Management for financial support. Partial support also has been obtained from Health Ministry and ISPESL through the strategic project titled: "Metodologie innovative per la valutazione del rischio da esposizione occupazionale a nanomateriali". The authors are very grateful to Dr. Paolo Prosposito of the Physics Department of the University of Rome Tor Vergata for the absorption measurements.

References and Notes

(1) Greene, M. A. In *Third Generation Photovoltaics—Advanced Solar Energy Conversion*; Springer: Berlin, Germany, 2004.

(2) Nozik, A. J. *Phys. E* **2002**, *14*, 115.

(3) Klimov, V. I. *Phys. Rev. Lett.* **2004**, *92*, 186601.

(4) Keem, K.; Kim, H.; Kim, G. T.; Lee, J.-S.; Min, B.; Cho, K.; Sung, M.-Y.; Kim, S. *Appl. Phys. Lett.* **2004**, *84*, 4376.

(5) Kim, K.-H.; Keem, K.; Jeong, D.-Y.; Min, B.; Cho, K.; Kim, H.; Moon, B.-M.; Noh, T.; Park, J.; Suh, M.; Kim, S. *J. Appl. Phys.* **2006**, *45*, 4265.

(6) (a) Peng, K.; Xu, Y.; Wu, Y.; Yan, Y.; Lee, S.-T.; Zhu, J. *Small* **2005**, *1*, 1062. (b) Peng, K.; Wang, X.; Lee, S.-T. *Appl. Phys. Lett.* **2008**, *92*, 163103.

(7) Califano, M.; Franceschetti, A. *Appl. Phys. Lett.* **2004**, *84*, 2409.

(8) Kongkanand, A.; Tvrdy, K.; Takechi, K.; Kuno, M.; Kamat, P. V. *J. Am. Chem. Soc.* **2008**, *130*, 4007.

(9) Special issue on Carbon Nanotubes: *Acc. Chem. Res.* **2002**, *35*, 997.

(10) Kamat, P. V. *Nanotoday* **2006**, *1*, 20.

(11) (a) Hirsch, A. *Angew. Chem.* **2002**, *114*, 1933. (b) Hirsch, A. *Angew. Chem., Int. Ed.* **2002**, *41*, 1853.

(12) (a) Tagmatarchis, N.; Prato, M. *J. Mater. Chem.* **2004**, *14*, 437. (b) Guldi, D. M.; Rahman, G. M.; Zerbetto, F.; Prato, M. *Acc. Chem. Res.* **2005**, *38*, 871.

(13) Lee, J. U. *Appl. Phys. Lett.* **2005**, *87*, 073101.

(14) Barazzouk, S.; Hotchandani, S.; Vinodgopal, K.; Kamat, P. V. *J. Phys. Chem. B* **2004**, *108*, 17015.

(15) Zhang, Y.; Gong, T.; Liu, W.; Zhang, X.; Chang, J.; Wang, K.; Wu, D. *Appl. Phys. Lett.* **2005**, *87*, 173114.

(16) Castrucci, P.; Tombolini, F.; Scarselli, M.; Speiser, E.; Del Gobbo, S.; Richter, W.; De Crescenzi, M.; Diociaiuti, M.; Gatto, E.; Venanzi, M. *Appl. Phys. Lett.* **2006**, *89*, 253107.

(17) De Crescenzi, M.; Tombolini, F.; Scarselli, M.; Speiser, E.; Castrucci, P.; Diociaiuti, M.; Casciardi, S.; Gatto, E.; Venanzi, M. *Surf. Sci.* **2007**, *601*, 2810.

(18) Robel, I.; Bunker, B.; Kamat, P. V. *Adv. Mater.* **2005**, *17*, 2458.

(19) Vietmeyer, F.; Seger, B.; Kamat, P. V. *Adv. Mater.* **2007**, *19*, 2935.

(20) Aminur Rahman, G. M.; Guldi, D. M.; Zambon, E.; Pasquato, L.; Tagmatarchis, N.; Prato, M. *Small* **2005**, *1*, 527.

(21) Cho, Y.; Kim, C.; Moon, H.; Choi, Y.; Park, S.; Lee, C. K.; Han, S. *Nano Lett.* **2007**, *8*, 81.

(22) Androitis, A. N.; Menon, M.; Froudakis, G. E. *Appl. Phys. Lett.* **2000**, *76*, 3890.

(23) (a) Bittencourt, C.; Felten, A.; Ghijsen, J.; Pireaux, J. J.; Drube, W.; Enri, R.; Van Tendeloo, G. *Chem. Phys. Lett.* **2007**, *436*, 368. (b) Bittencourt, C.; Felten, A.; Douhard, B.; Colomer, J.-F.; Van Tendeloo, G.; Drube, W.; Ghijsen, J.; Pireaux, J. J. *Surf. Sci.* **2007**, *601*, 2800.

(24) Xue, B.; Chen, P.; Hong, Q.; Lin, J.; Tan, K. L. *J. Mater. Chem.* **2001**, *11*, 2378.

(25) Kong, K.; Han, S.; Ihm, J. *Phys. Rev. B* **1999**, *60*, 6074.

(26) (a) De Crescenzi, M.; Diociaiuti, M.; Lozzi, L.; Picozzi, P.; Santucci, S. *Solid State Commun.* **1990**, *74*, 115.

(27) Di Nardo, S.; Lozzi, L.; Passacantando, M.; Picozzi, P.; Cantucci, S.; De Crescenzi, M. *Surf. Sci.* **1994**, *307309*, 922.

(28) The IPCE (photon-to-current efficiency) was determined by using the following equation: IPCE(%) = [100 × i(A/cm^2) × 1240]/[I(W/cm^2) × λ(nm)], where i is the short circuit photocurrent (A/cm^2), I is the incident light intensity (W/cm^2,) and λ is the incident wavelength (nm). For details see: Khazraji, A. C.; Hotchandani, S.; Das, S.; Kamat, P. V. *J. Phys. Chem. B* **1999**, *103*, 4693.

(29) Guldi, D. M.; Rahman, G. M. A.; Prato, M.; Jux, N. J.; Qin, S.; Ford, W. *Angew. Chem., Int. Ed.* **2005**, *44*, 2015.

(30) Hasobe, T.; Murata, H.; Kamat, P. *J. Phys. Chem. C* **2007**, *111*, 16626.

(31) Moulder, J. F.; Stickle, W. F.; Sobol, P. E. *Handbook of X-Ray Photoelectron Spectroscopy*; Perkin-Elmer, Physical Electronics Division, 1993.

(32) Shirley, D. A. *Phys. Rev. B* **1972**, *5*, 4709.

(33) Kuhn, H. J.; Braslavsky, S. E.; Schmidt, R. *Pure Appl. Chem.* **1989**, *61*, 187.

(34) Shyu, F. L.; Lin, M. F. *Phys. Rev. B* **2000**, *62*, 8508.

(35) (a) Mohite, A.; Sumanasekera, G. U.; Hirahara, K.; Bandow, S.; Iijima, S.; Alphenaar, B. W. *Chem. Phys. Lett.* **2005**, *412*, 190. (b) Mohite, A.; Chakraborty, S.; Gopinath, P.; Sumanasekera, G. U.; Alphenaar, B. W. *Appl. Phys. Lett.* **2005**, *86*, 61114.

(36) Fuhrer, M. S.; Nygård, J.; Shih, L.; Forero, M.; Yoon, Y.-G.; Mazzoni, M. S. C.; Choi, Y. J.; Ihm, J.; Louie, S. G.; Zettl, A.; McEuen, P. L. *Science* **2000**, *288*, 494.

JP809944D